Characterization of a novel conformational GII.4 norovirus epitope: Implications in norovirus-host interactions

Noelia Carmona-Vicente[1]§, Susana Vila-Vicent[1]§, David Allen[2,3], Roberto Gozalbo-Rovira[1], Miren Iturriza-Gómara[3,4], Javier Buesa[1,5]* and Jesús Rodríguez-Díaz[1,5]*

[1]Department of Microbiology, School of Medicine, University of Valencia, Avda. Blasco Ibáñez 17, 46010 Valencia, Spain; [2]Virus Reference Department, Public Health England, London, UK; [3]NIHR Health Protection Research Unit in Gastrointestinal Infections, University of Liverpool, UK; [4]Institute of Infection and Global Health, University of Liverpool, Liverpool, UK; [5]Institute for Clinical Research of the Hospital Clínico Universitario (INCLIVA) Valencia, Spain

§These two authors contributed equally to this work

*To whom correspondence should be addressed:
Department of Microbiology, School of Medicine, University of Valencia,
Avda. Blasco Ibáñez 17, 46010 Valencia, Spain
Email: jesus.rodriguez@uv.es or javier.buesa@uv.es
Phone: +34 963864903 or +34963864658
Fax: +34 963864960

RUNNING TITLE: A novel conformational GII.4 norovirus capsid epitope

ABSTRACT

Human noroviruses (NoVs) are the main etiological agents of acute gastroenteritis worldwide. While NoVs are highly diverse (more than 30 genotypes have been detected in humans), during the last 40 years most outbreaks and epidemics have been caused by GII.4 genotype strains, raising questions about their persistence in the population. Among other potential explanations, immune evasion is considered to be a main driver for their success. In order to study antibody recognition and evasion in detail, we have analyzed a conformational epitope recognized by a monoclonal antibody (3C3G3) by phage display, site-directed mutagenesis and surface plasmon resonance. Our results show that the predicted epitope is composed of eleven amino acids within the P domain: P245, E247, I389, Q390, R397, R435, G443, Y444, P445, N446, and D448. Only two of them, R397 and D448, differ from the homologous variant (GII.4 Den-Haag_2006b) and from a previous variant (GII.4 VA387_1996) which is not recognized by the antibody. A double mutant derived from the VA387_1996 variant containing both changes Q396R and N447D is recognized by the 3C3G3 monoclonal antibody, confirming the participation of these two sites in the epitope recognized by this antibody. Furthermore, a single change, Q396R, is able to modify the HBGA recognition pattern. These results provide evidence that the epitope recognized by the 3C3G3 antibody is involved in the virus-host interactions both at the immunological, as well as at the receptor levels.

KEY WORDS: Norovirus, GII.4 genotype, epitope, monoclonal antibody, virus-host interaction, viral variant, antibody escape, receptor

47

48 **IMPORTANCE**

49 Human noroviruses are the main cause of viral diarrhea worldwide in people of all
50 ages. Noroviruses can infect individuals who had been previously exposed to the
51 same or different norovirus genotypes. Norovirus genotype GII.4 has been reported to
52 be the most prevalent during the last 40 years. In the present study, we describe a
53 novel viral epitope identified by a monoclonal antibody and located within the highly
54 diverse P domain of the capsid protein. The evolution of this epitope along sequential
55 GII.4 variants has allowed noroviruses to evade previously elicited antibodies, thus
56 explaining how the GII.4 genotype can persist over long periods, re-infecting the
57 population. Our results also show that this epitope participates in the recognition of
58 host receptors which have evolved over time as well.

59

60

INTRODUCTION

Noroviruses (NoVs) are the predominant etiological agents of acute gastroenteritis worldwide, causing both outbreaks and sporadic cases (1-3). NoVs have become in many countries the main cause of infantile gastroenteritis since the introduction of rotavirus vaccines (4-7), and they have also been recognized globally as the main cause of associated foodborne diseases (8, 9).

NoVs belong to the *Caliciviridae* family, and currently they are classified into 6 genogroups (GI-GVI) (10) subdivided into more than 30 genotypes based on the capsid protein sequence diversity. That notwithstanding, most human NoV infections are caused by genogroups GI and GII. Furthermore, in the last two decades genotype GII.4 has been the causative agent of >95% of NoV gastroenteritis outbreaks, with globally distributed epidemic viral variants emerging every 2-3 years (11, 12).

NoVs are small non-enveloped viruses with a non-segmented single-stranded positive-sense RNA genome, which encodes the viral structural and non-structural proteins in three open reading frames (ORFs). ORF1 encodes the six non-structural proteins, including the viral protease and the RNA-dependent RNA polymerase (RdRp), while ORF3 encodes a small basic protein, VP2, which interacts with the VP1 and stabilizes the virion (13). ORF2 encodes the major structural protein VP1, which is further organized into the N-terminal (N), the shell (S), and the protruding (P) domains. The P domain can be further divided into two subdomains, P1 and P2 (14). The P1 subdomain forms the anchoring portion of the P dimer, connecting it to the S domain and promoting the stability of the viral particle, while the P2 subdomain is exposed on the surface of the capsid protein and is the most variable region of the virus (11). Both the main epitopes for immunorecognition, as well as the histo-blood group antigen (HBGA) binding domains, reside within this P2 subdomain. The

emergence and accumulation of mutations along the P2 subdomain is the main driver of evolution for GII.4 strains, and results in new epidemic strains with altered antigenicity and HBGA binding properties (15-18).

GII.4 genotypes associated with the majority of NoV pandemics have been GII.4 US1995_1996, Farmington_Hills_2002, GII.4 Hunter_2004, GII.4 Den Haag_2006b, GII.4 New Orleans_2009, and most recently GII.4 Sydney_2012. Of these six pandemic strains, it has been postulated that the first four are the result of the mutational evolution of the P domain capsid, whereas the two most recent variants display additional recombination events between ORF1 and ORF2 (12, 19).

Despite recent advances in norovirus culture *in vitro* (20), the historical lack of an *in vivo* model (which mimics the disease) and of a reproducible *in vitro* replication system have hampered the study of NoVs including a definitive explanation to the evolutionary success of GII.4 strains. Despite these challenges, several alternatives and surrogate systems have been successfully applied to the study of the immunogenicity and receptor binding properties of NoV strains and their variants. Virus-like particle (VLP) expressed in mammalian or insect cells (21) and P particles expressed in *E. coli* (22) show similar structural properties to the native virus, maintain the antigenic properties and HBGA binding ability, and their use has led to the identification of several epitopes and HBGA binding domains (15, 23-26).

In order to further characterize the impact of NoV GII.4 evolution on immune evasion, we analyzed the functionality of the epitope recognized by a monoclonal antibody (3C3G3) directed against a NoV GII.4 strain, using phage display and site-directed mutagenesis. The epitope recognized is composed of eleven amino acids, two

of them, R397 and D448, being implicated in the folding of the epitope and in the recognition patterns for different HBGAs.

MATERIALS AND METHODS

Expression and purification of norovirus virus-like particles (NoV VLPs)

VLPs of NoV strains GI.1 Norwalk, GII.3, GII.4_1999 (v0), GII.4_2004 (v2) and GII.4 Den Haag_2006b were expressed in insect cells after infection with recombinant baculoviruses, as previously described (15).

Expression and purification of recombinant NoVs P particles and P domains

P particles from NoV GI.1 Norwalk strain, GII.9 VA207 strain and GII.4 variants VA387_1996, Den Haag_2006b and Sydney_2012, as well as five mutants of the VA387_1996 variant (M1 to M5, see below) were produced and purified in *E. coli* BL21 as previously described (27). GII.9 VA207 synthetic gene was purchased as a synthetic gene (GeneArt, Invitrogen). The Den Haag_2006b P particle was subcloned from a previous VP1 construction available in our laboratory (28) using the primers P524 and P590 previously described (22), and the GII.4 Sydney_2012 variant was cloned from a clinical sample using P-Sydney forward (5'GCACGGATCCTCAAGAACTAAACCATTCTCTG3') and reverse (5'GCATGCGGCCGCTTAGCAAAAGCAATCGCCACGGCAATCGCATACTGC ACGTCTACGCCCCGTTCC3') primers. The P domain of the GII.4 Apeldoorn_2007 strain was also produced and purified as previously described (28). This construction is referred to as P domain and not P particle because it lacks the cysteine rich peptide that stabilizes the formation of P particles.

After the affinity chromatography step 10 mM EDTA was added to the resulting P particles to chelate the co-eluted nickel and loaded into a preparative HiPrep 16/60 Sephacryl S-300 HR size exclusion chromatography column (GE Healthcare Life Sciences, Uppsala, Sweden) equilibrated with PBS. The fractions corresponding to the P particles (molecular weights between 750 and 1,100 kDa) were pulled and stored at -20ºC in PBS containing 10% glycerol.

Antibodies utilized in the present study

A newly developed monoclonal antibody (3C3G3 mAb) was obtained by immunizing a six-week-old female BALB/c mouse with NoV VLPs from GII.4 Den Haag_2006b via intraperitoneal injection with Freund's adjuvant. Three days after the final boost injection, mouse spleen lymphocytes were fused with Sp2/0-Ag14 myeloma cells and hybridomas were screened by ELISA and subcloned by limiting dilution. One of the growing hybridomas produced an anti-GII.4_2006b VLP mAb (3C3G3) which was purified using HiTrap protein A sepharose columns (GE Healthcare). Two previously obtained and characterized monoclonal antibodies were also used in the present study: the anti-v0.8 mAb raised against the pre-epidemic GII.4 v0_2000 variant, and the anti-v2.5 mAb raised against the GII.4 v2_2004 variant (15). Two polyclonal antisera were also utilized in the present study. These were obtained by immunizing rabbits following standard methods, either with GII4 VA387_1996 P particles (P-pAb) or with a mixture of VLPs GII.4 v0_2000, GII.4 v2_2004 and GII.3 (HPA-pAb).

Characterization of antibodies by ELISA

156 The 96-well microtiter plates (Corning, NY) were coated with the different VLP
157 variants, P particles or P domain (see above) at 1 µg/ml in carbonate/bicarbonate
158 buffer (pH 9.2) and incubated overnight at 4ºC. Plates were blocked by incubating 1 h
159 at 37ºC in PBS 0.05% Tween (PBST) with 3% BSA. The primary antibodies (anti-
160 v0.8 mAb, anti-v2.5 mAb, 3C3G3 mAb, P-pAb and HPA-pAb were added to the
161 coated plates at two fold dilutions starting at 1/1,000 until 1/128,000 dilution in PBST
162 containing 1% BSA. Binding was detected with either HRP-conjugated anti-mouse
163 IgG at 1/4,000 or anti-rabbit IgG at the same dilution (Santa Cruz Biotechnology) as
164 appropriate. The reactions were developed by the addition of OPD (*o*-
165 phenylenediamine dihydrochloride, Sigma) and stopped after 10 min of incubation
166 with 3 M H_2SO_4. Absorbance was measured at 492 nm in a microplate reader
167 Multiskan Spectrum (Thermo Fisher Scientific, Vantaa, Finland). Assays were
168 performed in triplicate and negative and blank controls were included. The mean
169 value of negative controls (without primary antibody) plus 3 SDs was used as the cut-
170 off value.

171 **Saliva binding blocking assay**

172 Microtiter plates (Corning, NY) were coated with saliva from one secretor positive
173 donor diluted 1/500 in carbonate/bicarbonate buffer (pH 9.2), and incubated 37ºC for
174 1 h and at 4ºC overnight. Plates were washed three times with PBST and blocked with
175 PBS containing 3% BSA for 1 h at 37ºC. The GII.4 2006b P particles (1 µg/ml) were
176 incubated 1 h with serial dilutions of the 3C3G3 mAb in PBST at 37ºC. The mixture
177 was added to the coated plate and incubated for 1 h at 37ºC. After three washes, the P-
178 pAb was added at a dilution of 1/1,000. Finally, a HRP-conjugated anti-rabbit at
179 1/4,000 (Santa Cruz Biotechnology) was added. The OPD substrate was used to
180 develop the reactions that were stopped after a 20 min by adding 3 M H_2SO_4. The

absorbance was measured at 492 nm. Assays were performed in triplicate and the blocking of the binding was expressed as percentages of signal referred to the negative blocking control OD_{492} (P particles without any blocking agent).

3C3G3-epitope characterization by phage display

Ph.D.-C7C Phage Display Peptide Libraries ($1.5x10^{13}$ plaque forming units (pfu)/ml) and the host bacterial strain *E. coli* ER2738 were purchased from New England Biolabs (Beverly, MA, USA).

Panning was carried out in 96-well microtiter plates by direct target coating, mainly referenced from the Ph.D.-C7C library kit manual. Briefly, purified 3C3G3 mAb (100 µg/ml) was coated on a 96-well plate with 150 µl of carbonate buffer (0.1M NaHCO3, pH 8.6) and incubated overnight at 4°C under gentle agitation. Nonspecific binding was blocked by incubation with 300 µl of blocking buffer (NaHCO3 0'1 M pH 8'6 containing BSA at 5 mg/ml) for 1 h at 4°C. For the panning–elution procedure, approximately 2×10^{11} pfu/ml phages diluted with 0.1% TBST were incubated with the 3C3G3-coated plate for 45 min at room temperature with shaking. Unbound phages were removed by washing with 0.01% TBST. The 3C3G3 mAb-bound phages were eluted with 100 µl of glycine (0.2 M glycine-HCl, pH 2.2) containing 1 mg/ml of BSA and then neutralized with 15 µl of Tris-HCl 1 M pH 9.1. The eluted phages were amplified and purified to be used for subsequent rounds of selection and to infect *E. coli* ER2738 for amplification and titration. In the second and third rounds of panning, the stringency of washing was augmented by increasing the number of washes and the amount of Tween-20, in consecutive rounds.

After three rounds of panning–elution selection, individual positive clones were picked up from LB/IPTG/Xgal plates, amplified and submitted for DNA sequencing.

206 The primer used for sequencing was 96gIII (5′-CCCTCATAGTTAGCGTAACG-3′),
207 provided by the kit. The sequences coding 7 amino acids were identified and used to
208 predict the epitope.

209

210 **Epitope modeling**

211 Conformational modeling of the epitope was carried out using the Pepitope server
212 (29). The crystal structure of the NoV GII.4 VA387_1996 strain was used as the
213 model to localize the epitope recognized by mAb 3C3G3 (PDB id: 2OBR). The
214 Modeller (http://salilab.org/modeller/) program (version 9.15) was used for homology
215 and comparative modeling of three-dimensional protein structures (30). We used the
216 GII.4 VA387_1996 strain structure as the template (PDB id: 2OBR) and provided an
217 adequate alignment with the sequences of the different mutants M1 to M5 (see
218 below). The Modeller software built the required number of models of the target and
219 estimated the quality parameters of the models. The model with the best dope score
220 was chosen for each mutant. The structures were visualized with the Pymol (The
221 PyMol Molecular Graphics System, Version 0.99, Schrodinger, LLC) program.

222

223 **Site-directed mutagenesis**

224 To confirm the amino acid residues forming part of the 3C3G3 epitope, the GII.4
225 VA387_1996 strain (not recognized by the antibody) was used as a scaffold to
226 incorporate the amino acids present in the predicted epitope. Five mutants were
227 constructed by introducing the following mutations into the GII.4 VA387_1996
228 sequence: M1 (Q396R); M2 (N447D); M3 (NN- 393, 394 STT); M4 (M1+M2); and
229 M5 (M1+M2+M3) (Figure 1). The GeneArt site-directed mutagenesis system

(Thermo Fisher) was applied following the manufacturer's instructions to incorporate the mutations. The primers utilized to create the mutants are listed in Table 1. M1 and M2 were produced in one step, but M3 was constructed in two steps using first the MUT_3_1_FW and MUT_3_1_RV primers and then the MUT_3_2_FW and MUT_3_2_RV in a second mutagenesis reaction. The M4 construction (double mutant incorporating M1 and M2) was made using the M1 construction as the template and incorporating the M2 mutation afterwards. To create the M5 mutant, the M3 construction was used as template using primers MUT_1_3_FW and MUT_1_3_RV to incorporate M1 without changing the M3 mutation that was already present, followed by the addition of the M2 mutation.

Transformants were analyzed by PCR and sequencing. Positive transformants were transferred to the *E.coli* BL21 strain GroES/EL and mutant P particles were produced and purified as previously described (27).

Surface plasmon resonance (SPR)

The binding ability of P particles (GII.4 VA387_1996, M1, M2, M3, M4, M5 and Den Haag_2006b) to three different mAbs (3C3G3, anti-V0.8 and anti-V2.5) was tested by Surface Plasmon Resonance (SPR) using a Biacore T100 instrument (Biacore, GE Healthcare). An anti-His antibody (Clontech) was immobilized on the surface of CM5 chips (GE Healthcare) and used as a capture antibody for P particles. Immobilization was achieved using the Amine Coupling Kit (GE Healthcare). Briefly, 5000 anti-His mAb resonance units (RU) were immobilized in channel 2 leaving channel 1 as a reference. Each P particle was captured flowing a solution of 100 µg/ml for 100 seconds at a flow rate of 5 µl/min in HBS-EP$^+$ buffer (GE Healthcare) to reach a capture level of ~100 RUs. Several dilutions of each mAb (100 nM, 50 nM,

25 nM, 12.5 nM and 6.125 nM) were injected, starting with the most dilute and finishing with the most concentrated one, on the CM5 chip at a flow rate of 30 µl/min in HBS-EP$^+$ buffer (GE Healthcare) at 25ºC in single cycle kinetics experiments. The binding time was 60 seconds with final dissociation time of 600 seconds. Each interaction was tested in three independent experiments. Binding and kinetics evaluations were performed with the Biacore Evaluation Software.

P particle binding to neoglycoconjugates

The binding of P particles to five different neoglycoproteins (Table 2) with the oligosaccharide structure of antigen H (blood group O), of blood group A, blood group B, Lewis X (Le^x) and Sialyl Lewis X (SiLe^x) was assayed by ELISA. All the neoglycoproteins were obtained from Isosep AB (Tullinge, Sweden). The oligosaccharides were linked to human serum albumin (HSA), through an acetylphenylenediamine (APD) or aminophenylethyl (APE) spacer, with 10–30 oligosaccharides per protein molecule.

Microtiter plates (Corning, NY) were coated with the different neoglycoconjugates at 1 µg/ml in carbonate/bicarbonate buffer (pH 9.2), and incubated 37ºC for 1 h and at 4ºC overnight. Plates were washed three times with PBST and blocked with PBS containing 3% BSA for 1 h at 37ºC. The P particles were added at 1 µg/ml in PBST and the plates were incubated 90 min at 37ºC. After three washes, the P-pAb was added to the plates at a dilution of 1/1,000. Binding was detected with HRP-conjugated anti-rabbit at 1/ 4,000 (Santa Cruz Biotechnology). The reactions were developed by the addition of OPD and stopped after a 20 min incubation with 3 M H_2SO_4. Absorbance was measured at 492 nm. Assays were performed in triplicate and

negative (non-functionalized HSA at 1 μg/ml), and blank controls were included. The binding was expressed as percentages of signal referred to the higher OD_{492}.

Ethics statement

In this study, Balb/c mice were employed to obtain monoclonal antibodies. The Animal Welfare and Ethics Committee of the University of Valencia approved all the protocols conducted here, according to applicable national and international guidelines. JB possesses the accreditation by the Conselleria de Agricultura, Generalitat Valenciana, to design and perform experiments with laboratory animals.

288 **RESULTS**

289 **Production and purification of norovirus P particles**

290 With the aim to study the immunogenicity and binding ability of different NoV strains
291 to several HBGAs a total of ten P particles were produced, one corresponding to the
292 GI.1 Norwalk genotype, four corresponding to different GII NoVs (GII.9 VA207
293 strain, GII4 VA387_1996 strain, GII.4 Den Haag_2006b strain and GII4
294 Sydney_2012 strain), and the remaining obtained by site-directed mutagenesis of the
295 GII.4 VA387_1996 P particle (M1 to M5). All the proteins showed a molecular
296 weight close to the expected one (36 kDa), but with small differences. The GII4
297 VA387_1996 variant showed a typical duplet band for this strain (22, 27). This duplet
298 was also present in the M1 (Q396R) mutant. The M2 mutant (N447D) migrated as a
299 single band, as well as did all the other constructions, except the M4 double mutant
300 that displayed a lower mobility in the gel (Figure 2). The P particles were further
301 purified by size exclusion chromatography. The results showed that the majority
302 (more than 80%) of the produced proteins formed particles as it can be observed in
303 Figure 3. The elution time was slightly different for every preparation ranging from
304 37.89 ml (M1) to 40.29 ml (VA387) that corresponds to 1,030 kDa to 870 kDa
305 (Figure 3). All together we were able to produce and purify ten different P particles
306 that were used in ELISA, SPR and binding assays.

307

308 **Characterization of mAb by ELISA**

309 In order to elucidate the reactivity patterns of each one of the mAbs against different
310 NoV genogroups, genotypes and variants the initial characterization of mAbs 3C3G3,
311 anti-v0.8 and anti-v2.5 was performed by ELISA using a set of NoV antigens (Table 3

and Figure 4). As a control, the HPA-pAb was utilized. The 3C3G3 antibody recognized only its homologous VLP (GII.4 Den Haag_2006b) and the most closely related GII.4 Apeldoorn_2007 P domain. Surprisingly, it did not recognize the GII.4 v2_2004 VLPs and GII.4 VA387_1996 P particle, two different variants within the same genotype. This result is similar to those obtained with the anti-v0.8 and anti-v2.5 mAbs. The anti-v0.8 efficiently recognized its homologous GII.4 v0_1999 VLP and the GII.4 VA387_1996 P particle while the anti-v2.5 recognized only its homologous GII.4 v2_2004 VLP and the closer GII.4 2006b antigen, but not the GII.4 Apeldoorn_2007 P domain. The HPA polyclonal antibody was able to recognize all the tested antigens except the GI.1 P particles (Table 3). These results confirm that the fast evolution of NoV GII.4 variants seem to be driven by the antibody pressure in the host, favoring the emergence of antibody escape variants.

The 3C3G3 mAb blocks the binding of P particles to saliva

The main aim of the present study was to characterize the epitope of a mAb directed to the viral capsid protein to give an explanation on how antibody evasion occurs in NoV GII.4 variants. It was important to know if the 3C3G3 mAb was able to block the binding of NoV to its receptors. For this reason a saliva binding blocking assay was performed, and the results confirmed that the 3C3G3 mAb is able to block the binding of GII.4 Den Haag_2006b P particles in a dose dependent manner to secretor positive saliva (Figure 5).

Characterization of the 3C3G3 mAb epitope by phage display and site-directed mutagenesis

Aiming to characterize the epitope recognized by the 3C3G3 mAb the phage display technique followed by site-directed mutagenesis were applied. After three rounds of panning, a consensus sequence of 11 amino acids was obtained. The predicted epitope was formed by the following amino acids: P245, E247, I389, Q390, R397, R435, G443, Y444, P445, N446, and D448 of the GII.4 Den Haag_2006 variant (Figure 1). Three of these amino acids are within the P2 subdomain (I389, Q390, R397), and the other eight are within the P1 subdomain (Figure 6).

To confirm the epitope, site-directed mutagenesis was performed using the P particle of GII.4 VA387_1996 variant as a scaffold. This variant was not recognized by the 3C3G3 mAb, and only two residues were different among both proteins in the predicted epitope R397 and D448 (Figure 1). Five mutants were produced as described in the Material and Methods section (M1 (Q396R); M2 (N447D); M3 (NN-393, 394 STT); M4 (M1+M2) and M5 (M1+M2+M3)), and the reactivity of the 3C3G3 mAb against the mutants was tested by ELISA. In addition to the mutants, two new P particles were added to the experiment: The GII.4 Den Haag_2006 variant P particles as the positive control and the GII.4 Sydney_2012 variant P particles to evaluate the performance of the antibody towards the newer GII.4 epidemic variant. The ELISA results, summarized in Table 3 and Figure 7A, found that none of the single mutants M1, M2, or M3 were recognized by the antibody. Interestingly, both the double mutant M4 and the multiple mutant M5 were recognized by the antibody, thus confirming that at least R397 and D447 form part of the epitope recognized by the 3C3G3 antibody. These results show that the antigenic site B (STT 393,394,395) does not seem to be involved in the formation of the 3C3G3 epitope, since M3 was

not recognized by the 3C3G3 mAb. It is also interesting that the later epidemic variant GII.4 Sydney_2012 is not recognized by the mAb while it shares the 11 residues of the predicted epitope (Table 4). This indicates that other residues not identified in this study might be implicated in the formation of the 3C3G3 epitope.

To know if this novel described epitope affects the binding of other GII.4 directed mAbs the reactivity of anti-v0.8 and anti-v2.5 mAbs against the different P particles was also assayed by ELISA. The results show that the anti-v2.5 epitope might be different from the 3C3G3 epitope since none of the mutants were recognized by this mAb (Figure 7B). Interestingly this antibody was also independent from the previously described antigenic site B present here in M3 and M5 constructions (15). In contrast, the anti-v0.8 mAb reacted against each of the mutants, albeit at different levels. This may indicate that the selected residues exert an influence on the folding of the epitope recognized by this antibody since both mutagenized residues are conserved in VA387_1996 and V0_1999 variants (Table 4). According to our results this mAb showed a dependence on the antigenic B site as previously described (15).

Characterization of the 3C3G3 mAb-epitope by surface plasmon resonance

To quantify the interaction strength between the tested mAbs and the different P particles recognized by them, a surface plasmon resonance (SPR) approach was applied and affinity constants (KD) were obtained in at least three independent experiments. Of all the interaction pairs, the highest affinity (lowest KD value) was obtained in the 3C3G3- GII4 Deen Hag_2006b interaction pair (Table 3 and Figure 8). Although M4 gave higher signal in ELISA (Figure 7A), the SPR experiments revealed that the M4 mutant had 6 times higher KD (153 nM) than M5 mutant did (25

nM) (Table 3). After modeling the structure of the different mutants, using the P domain of VA387_1996 structure as a scaffold (PDB id: 2OBR), we observed that the R397 and the D448 residues probably present different conformations in M4 and M5 (Figures 3C and D). The M5 model had the D448 anionic carboxylate ($RCOO^-$) and R397 cationic ammonium ($RNH3^+$) closer. This increased the possibility of a saline bridge formation that permitted the 3C3G3 epitope stabilization.

R397 is involved in HBGAs recognition

The binding of the VA387_1996, Den Haag_2006b and Sydney_2012 variants, as well as of the five mutants (M1 to M5) to five different HBGAs ($SiLe^x$, Le^x, blood group O (H antigen), blood group A and blood group B) was analyzed in order to study if the residues involved in their immunogenicity also had an impact in their receptor binding. Our results show that there was a change in the recognition pattern between the VA387_1996 and the Den Haag_2006b and Sydney_2012 variants. While the VA387_1996 strain possessed a high binding ability to the $SiLe^x$ antigen, the Den Haag_2006b and Sydney_2012 variants did not recognize any of the assayed antigens (Figure 9). Interestingly, the M1 incorporating the single mutation Q396R lost its binding ability to the tested HBAs, showing the same recognition pattern as the 2006b and 2012 variants. The M2 mutant maintained a similar binding to $SiLe^x$ as did the wild type VA387_1996. M3 and M4 increased their recognition ability to blood group A, B and O antigens. Moreover, M4 recognized the non-functionalized HSA. Finally, the M5 mutant demonstrated a residual binding of 10% to $SiLe^x$.

406 **DISCUSSION**

407 Due to the relevance of the antibody escape variants in NoV GII.4 persistence during
408 the last 40 years, we decided to resolve the epitope recognized by the 3C3G3 mAb,
409 which is a binding blocking antibody. The results of the present study shed light on
410 how NoV escapes to antibody neutralization. This antibody was not able to recognize
411 any of the tested antigens by Western Blot, indicating that the target epitope should be
412 conformational. For this reason, a phage display approach was chosen. Of the eleven
413 residues suspected to form part of the epitope (see Results) two of them, R397 and
414 D448, were confirmed to be part of the epitope by site-directed mutagenesis of
415 VA387_1996 P particles. When different P particles were produced, differences in
416 electrophoretic mobility were observed. These differences in the electrophoretic
417 mobility have been previously reported for the VA387 variant and were associated to
418 P particle formation (P dimers versus P particles) (22) and might reveal structural
419 changes. In the present study, all the designed P particles were found to be
420 successfully constructed, with estimated molecular weights ranging from 870 to 1,030
421 kDa.

422 Besides the R397 and D448 residues, another difference between VA387_1996 and
423 Den Haag_2006b sequences was a change involving amino acids 393-395 (STT in the
424 Den Haag_2006b variant and N-N in the VA387_1996 variant). This change was
425 incorporated in the M3 and M5 mutants because they were in the close vicinity of
426 R397. They had been previously described to form an important epitope in GII.4
427 NoVs (15). Nevertheless, these three residues did not rescue the binding ability of the
428 3C3G3 antibody (M3 was not recognized by 3C3G3), but they helped stabilizing the
429 3C3G3 epitope, since 3C3G3 had 6 times more affinity for M5 than for M4. After the

molecular modeling of the 5 mutants (Figure 6), we could predict the formation of a saline bridge between R397 and D448 only in M5 and not in M4. That could explain the higher stability of the 3C3G3 epitope in M5, while the 393-395 STT residues did not seem to be part of the 3C3G3 epitope themselves.

As shown in Table 4 it seems that residues R397 and D448 have been important in the successive GII.4 variants. In order to elucidate if they are part of epitopes recognized by other mAbs raised against different GII.4 variants we also characterized two previously obtained mAbs, anti-v0.8 and anti-v2.5, that were tested against the same antigens and mutants as 3C3G3 mAb. We confirmed by ELISA and SPR that the anti-v0.8 was dependent on antigenic site B (393-395 –NN to STT) as previously described (15). The epitope recognized by anti-v0.8 was also affected in the M1 and M2 mutants, indicating that amino acids 397 and 448 might also be implicated in the epitope conformation. Furthermore, the results with all three mAbs showed that there was only cross reactivity between the closer variants, and that none of the more distant variants shared any reactivity (Table 3). The anti-v2.5 mAb only recognized the more closely P particle corresponding to the GII.4 Den Haag_2006b variant. All the mutants were made using the VA387_1996 variant as scaffold that is not recognized by this antibody. Only if R397 and D448 were present in its epitope, recognition by this antibody would be recovered. The only conclusion that we can obtain is that these residues might not be part of the anti-v2.5 mAb epitope.

These results possess important implications from the evolutionary point of view, since they demonstrate that the mAbs against the older variants do not recognize the newer ones. They explain why the same genotype can produce successive pandemics. Moreover, the HPA-pAb is able to recognize the GI.1 VLPs, but not the GI.1 P

454 particles, supporting the idea that the cross-reactive epitopes between both NoV
455 genogroups are present only in the shell domain of VP1, which is not present in the P
456 particles (31, 32).

457 When the 3C3G3 epitope was compared in several NoVs GII.4 variants (Table 4), the
458 two residues identified in the present study, R397 and D448, were always conserved.
459 All the variants prior to 2004 possessed the combination Q397-N448, and all the
460 variants that emerged since 2006 contain the duplet R397-D448. There was a
461 transition period between 2004 and 2006 where both duplets were present, but always
462 in the same combination. In the VA387_1996 structure and in the structural models of
463 Figure 6 it was observed that these two amino acids were located very close to each
464 other, and in M5 they seemed to interact through a saline bridge. This physical
465 interaction might explain why these two residues were in fixed combinations
466 throughout the different variants. We could hypothesize that these residues might
467 additionally be involved in the stabilization of the P particle itself, not just in the
468 3C3G3 epitope. Indeed, we observed changes in the electrophoretic mobility of the
469 different P particles when these residues were mutagenized within the VA387_1996,
470 M1 and M4 P particles being the most heterogeneous migrating particles.
471 Nevertheless, the Den Haag_2006b and Sydney_2012 variants, which possess the
472 R397-D448 pair, along with the 393-395 STT version of the antigenic site B (that
473 favors the formation of the R397-D448 saline bridge), were more homogenous than
474 was the 1996 variant.

475 It is known that GII.4 noroviruses have strain specific HBGAs recognition patterns
476 (17, 18, 33). To evaluate whether the 3C3G3 epitope was involved in the interaction
477 with receptors, we analyzed the binding of the different GII.4 P particles to several
478 HBGAs. Our results indicated that the change in R397 seemed to be the key in the

479 different recognition patterns seen in the newer GII.4 variants compared to those of
480 the older ones. The conclusion reached was that this change might have had an effect
481 on the folding of the fucose-binding pocket that is not in contact with this residue
482 (Figure 6).

483 Interestingly, the M4 mutant that includes both substitutions (Q396R and N447D) has
484 an exacerbated binding ability including a high binding to the HSA (negative control).
485 In Table 4 we can observe that this amino acid combination (R396 and D447) is
486 always accompanied with the antigenic site B triplet and not with the duplet as it is
487 present in M4. The combination of the antigenic site B duplet with R396 and D447
488 has not been found in wild-type viruses so far, which may reflect a negative selection
489 process probably due to its impaired binding, as seen with M4 mutant.

490 This was the first time that phage display was applied to study GII.4 NoV epitopes. In
491 previous studies, evolutionary and structural approaches were used to identify
492 putative epitopes including site A (amino acids 296-298) and B (amino acids 393-
493 395) (16). These epitopes were confirmed using chimeras between different NoV
494 GII4 variants and monoclonal antibodies (15). A similar approach showed that site A
495 should be formed by amino acids 294, 368 and 372 in addition to 296-298 (17). It
496 whas also been shown that epitope B had an influence on the changes in the HBGA
497 binding abilities of different GII4 variants (17, 18). Using the phage display technique
498 we have been able to identify two residues (397 and 448) that were not as exposed as
499 the previously described epitopes, thus making it difficult to predict their relevance
500 after structural analysis. We have shown that these residues play an important role in
501 antibody recognition, HBGA interactions, and that they have evolved from ancestral
502 to modern variants.
503

Altogether, we were able to study the epitope recognized by the 3C3G3 antibody and have shown that this epitope was implicated in viral host interactions. On the one hand, the two amino acids, R397 and D448, seemed to be involved in the evasion to the host antibody response, showing how small changes in the amino acid sequence could render huge benefits to the virus in terms of antibody evasion. On the other hand, we have demonstrated that a single change in position 396 of the 1996 variant (397 of 2006b variant) could be enough to modulate the binding of noroviruses to HBGAs.

514 **AKNOWLEDGEMENTS**

515 This work was supported by the Ministry of Economy and Competitiveness
516 SAF2012-38368 to JB and AGL2014-52996-C2-2-R to JRD. NCV was the recipient
517 of a "V Segles" fellowship from the University of Valencia and JRD was the recipient
518 of a "Ramón y Cajal" contract from the Ministry of Economy and Competitiveness
519 (RYC-2013-12442).

520

REFERENCES

1. **Tam CC, Rodrigues LC, Viviani L, Dodds JP, Evans MR, Hunter PR, Gray JJ, Letley LH, Rait G, Tompkins DS, O'Brien SJ.** 2012. Longitudinal study of infectious intestinal disease in the UK (IID2 study): incidence in the community and presenting to general practice. Gut **61:**69-77.
2. **Gastanaduy PA, Hall AJ, Curns AT, Parashar UD, Lopman BA.** 2013. Burden of norovirus gastroenteritis in the ambulatory setting--United States, 2001-2009. The Journal of infectious diseases **207:**1058-1065.
3. **Patel MM, Widdowson MA, Glass RI, Akazawa K, Vinje J, Parashar UD.** 2008. Systematic literature review of role of noroviruses in sporadic gastroenteritis. Emerging infectious diseases **14:**1224-1231.
4. **Bucardo F, Lindgren PE, Svensson L, Nordgren J.** 2011. Low prevalence of rotavirus and high prevalence of norovirus in hospital and community wastewater after introduction of rotavirus vaccine in Nicaragua. PLoS One **6:**e25962.
5. **Williams DJ, Edwards KM, Payne DC, Manning J, Parashar UD, Lopman BA.** 2012. Decline in gastroenteritis-related triage calls after rotavirus vaccine licensure. Pediatrics **130:**e872-878.
6. **Koo HL, Neill FH, Estes MK, Munoz FM, Cameron A, DuPont HL, Atmar RL.** 2013. Noroviruses: The Most Common Pediatric Viral Enteric Pathogen at a Large University Hospital After Introduction of Rotavirus Vaccination. J Pediatric Infect Dis Soc **2:**57-60.
7. **Payne DC, Vinje J, Szilagyi PG, Edwards KM, Staat MA, Weinberg GA, Hall CB, Chappell J, Bernstein DI, Curns AT, Wikswo M, Shirley SH, Hall AJ, Lopman B, Parashar UD.** 2013. Norovirus and medically attended gastroenteritis in U.S. children. N Engl J Med **368:**1121-1130.
8. **Buesa J, Rodriguez Diaz J.** 2006. Molecular virology of enteric viruses (with emphasis on caliciviruses), p. 43-100. *In* Goyal S (ed.), Viruses in Foods. Springer, New York.
9. **Kirk MD, Pires SM, Black RE, Caipo M, Crump JA, Devleesschauwer B, Dopfer D, Fazil A, Fischer-Walker CL, Hald T, Hall AJ, Keddy KH, Lake RJ, Lanata CF, Torgerson PR, Havelaar AH, Angulo FJ.** 2015. World Health Organization Estimates of the Global and Regional Disease Burden of 22 Foodborne Bacterial, Protozoal, and Viral Diseases, 2010: A Data Synthesis. PLoS Med **12:**e1001921.
10. **Vinje J.** 2015. Advances in laboratory methods for detection and typing of norovirus. J Clin Microbiol **53:**373-381.
11. **Hoa Tran TN, Trainor E, Nakagomi T, Cunliffe NA, Nakagomi O.** 2013. Molecular epidemiology of noroviruses associated with acute sporadic gastroenteritis in children: global distribution of genogroups, genotypes and GII.4 variants. J Clin Virol **56:**185-193.
12. **White PA.** 2014. Evolution of norovirus. Clin Microbiol Infect **20:**741-745.
13. **Vongpunsawad S, Venkataram Prasad BV, Estes MK.** 2013. Norwalk Virus Minor Capsid Protein VP2 Associates within the VP1 Shell Domain. J Virol **87:**4818-4825.
14. **Prasad BV, Hardy ME, Dokland T, Bella J, Rossmann MG, Estes MK.** 1999. X-ray crystallographic structure of the Norwalk virus capsid. Science **286:**287-290.

15. **Allen DJ, Noad R, Samuel D, Gray JJ, Roy P, Iturriza-Gomara M.** 2009. Characterisation of a GII-4 norovirus variant-specific surface-exposed site involved in antibody binding. Virol J **6:**150.
16. **Allen DJ, Gray JJ, Gallimore CI, Xerry J, Iturriza-Gomara M.** 2008. Analysis of amino acid variation in the P2 domain of the GII-4 norovirus VP1 protein reveals putative variant-specific epitopes. PLoS One **3:**e1485.
17. **Debbink K, Donaldson EF, Lindesmith LC, Baric RS.** 2012. Genetic mapping of a highly variable norovirus GII.4 blockade epitope: potential role in escape from human herd immunity. J Virol **86:**1214-1226.
18. **Shanker S, Choi JM, Sankaran B, Atmar RL, Estes MK, Prasad BV.** 2011. Structural analysis of histo-blood group antigen binding specificity in a norovirus GII.4 epidemic variant: implications for epochal evolution. J Virol **85:**8635-8645.
19. **Eden JS, Tanaka MM, Boni MF, Rawlinson WD, White PA.** 2013. Recombination within the pandemic norovirus GII.4 lineage. J Virol **87:**6270-6282.
20. **Jones MK, Watanabe M, Zhu S, Graves CL, Keyes LR, Grau KR, Gonzalez-Hernandez MB, Iovine NM, Wobus CE, Vinje J, Tibbetts SA, Wallet SM, Karst SM.** 2014. Enteric bacteria promote human and mouse norovirus infection of B cells. Science **346:**755-759.
21. **Jiang X, Wang M, Graham DY, Estes MK.** 1992. Expression, self-assembly, and antigenicity of the Norwalk virus capsid protein. J Virol **66:**6527-6532.
22. **Tan M, Jiang X.** 2005. The p domain of norovirus capsid protein forms a subviral particle that binds to histo-blood group antigen receptors. J Virol **79:**14017-14030.
23. **Siebenga JJ, Vennema H, Renckens B, de Bruin E, van der Veer B, Siezen RJ, Koopmans M.** 2007. Epochal evolution of GGII.4 norovirus capsid proteins from 1995 to 2006. J Virol **81:**9932-9941.
24. **Tan M, Huang P, Meller J, Zhong W, Farkas T, Jiang X.** 2003. Mutations within the P2 domain of norovirus capsid affect binding to human histo-blood group antigens: evidence for a binding pocket. J Virol **77:**12562-12571.
25. **Lindesmith LC, Donaldson EF, Baric RS.** 2011. Norovirus GII.4 strain antigenic variation. J Virol **85:**231-242.
26. **Lindesmith LC, Donaldson EF, Lobue AD, Cannon JL, Zheng DP, Vinje J, Baric RS.** 2008. Mechanisms of GII.4 norovirus persistence in human populations. PLoS Med **5:**e31.
27. **Rubio-del-Campo A, Coll-Marques JM, Yebra MJ, Buesa J, Perez-Martinez G, Monedero V, Rodriguez-Diaz J.** 2014. Noroviral p-particles as an in vitro model to assess the interactions of noroviruses with probiotics. PLoS One **9:**e89586.
28. **Carmona-Vicente N, Fernandez-Jimenez M, Ribes JM, Tellez-Castillo CJ, Khodayar-Pardo P, Rodriguez-Diaz J, Buesa J.** 2015. Norovirus infections and seroprevalence of genotype GII.4-specific antibodies in a Spanish population. J Med Virol **87:**675-682.
29. **Mayrose I, Penn O, Erez E, Rubinstein ND, Shlomi T, Freund NT, Bublil EM, Ruppin E, Sharan R, Gershoni JM, Martz E, Pupko T.** 2007. Pepitope: epitope mapping from affinity-selected peptides. Bioinformatics **23:**3244-3246.

30. **Sali A, Blundell TL.** 1993. Comparative protein modelling by satisfaction of spatial restraints. J Mol Biol **234:**779-815.
31. **Parra GI, Azure J, Fischer R, Bok K, Sandoval-Jaime C, Sosnovtsev SV, Sander P, Green KY.** 2013. Identification of a Broadly Cross-Reactive Epitope in the Inner Shell of the Norovirus Capsid. PLoS One **8:**e67592.
32. **Crawford SE, Ajami N, Parker TD, Kitamoto N, Natori K, Takeda N, Tanaka T, Kou B, Atmar RL, Estes MK.** 2015. Mapping broadly reactive norovirus genogroup I and II monoclonal antibodies. Clinical and vaccine immunology : CVI **22:**168-177.
33. **Tan M, Xia M, Cao S, Huang P, Farkas T, Meller J, Hegde RS, Li X, Rao Z, Jiang X.** 2008. Elucidation of strain-specific interaction of a GII-4 norovirus with HBGA receptors by site-directed mutagenesis study. Virology **379:**324-334.

632 **Tables and Figure legends**

633

634 Table 1. Primers used for site-directed mutagenesis

Primer	Sequence	Mutant
MUT_1_FW	5'-CAGGATGGTAATAACCACAGGAATGAACCCCAGCAATG-3'	M1 and M4
MUT_1_RV	5'- CATTGCTGGGGTTCATTCCTGTGGTTATTACCATCCTG-3'	M1 and M4
MUT_2_FW	5'- CGGGTATCCCAACATGGACCTGGATTGCCTACTC-3'	M2, M4 and M5
MUT_2_RV	5'- GAGTAGGCAATCCAGGTCCATGTTGGGATACCCG-3'	M2, M4 and M5
MUT_3_1_FW	5'- CGTCATCCAGGATGGTAGCACCCACCAAAATGAACCCC-3'	M3 and M5
MUT_3_1_RV	5'- GGGGTTCATTTTGGTGGGTGCTACCATCCTGGATGACG-3'	M3 and M5
MUT_3_2_FW	5'- CCAGGATGGTAGCACAACCCACCAAAATGAACC-3'	M3 and M5
MUT_3_2_RV	5'-GGTCCTACCATCGTGTTGGGTGGTTTTACTTGG-3'	M3 and M5
MUT_1_3_FW	5'-CGTCATCCAGGATGGTAGCACAACCCACAGGAATGAACCCCAGCAATG-3'	M5
MUT_1_3_RV	5'-CATTGCTGGGGTTCATTCCTGTGGGTTGTGCTACCATCCTGGATGACG-3'	M5

635

636 Table 2. Neoglycoconjugates used in the present study

Designation	**Oligosaccharide structure**
H-type 1-HSA	Fucα2Galβ3GlcNAcβ3Galβ4Glcc-APD-
SiLe^x–HSA	Neu5Acα3Galβ4(Fucα3)GlcNAcβ3Galβ4Glcc-APD
Le^x–HSA	Galβ4(Fucα3)GlcNAcβ3Galβ4(Fucα3)GlcNAc-APD
A-tri-HSA	GalNAcα3(Fucα2)Galβ−O−APE
B-tri-HSA	Galα3(Fucα2)Galβ−O−APE

637

638

639

640

641 Table 3. Antibody reactivity against different norovirus antigens by ELISA and
642 affinity constants (KD) estimated by surface plasmon resonance.
643

Norovirus antigen	**Antibody**				
	HPA-pAb	P-pAb	3C3G3 mAb	Anti-v0.8 mAb	Anti-v2.5 mAb
VLP GI.1 Norwalk	+	ND	-	-	-
VLP GII.4-1999	+	+	-	+	-
VLP GII.4-2004	+	+	-	-	+
VLP GII.3	+	+	-	-	-
P-GI.1 Norwalk	-	ND	-	-	-
P-GII.4-1996	+	+	-	+ (47±35 nM)	-
P-GII.4-1996 M1	+	+	-	+ (72±49 nM)	-
P-GII.4-1996 M2	+	+	-	+ (7±1 nM)	-
P-GII.4-1996 M3	+	+	-	+ (12±3 nM)	-
P-GII.4-1996 M4	+	+	+ (153±74 nM)	+ (7±1 nM)	-
P-GII.4-1996 M5	+	+	+ (25±12 nM)	+ (12±3 nM)	-
P-GII.4-2006b	+	+	+ (2.1±1 nM)	-	+ (11±3 nM)
P-GII.4-2012	+	+	-	-	-
P-domain GII.4-2007	+	+	+	-	-

644 + = positive recognition; - = negative recognition; ND = not determined. HPA-pAb= rabbit
645 polyclonal anti-serum raised against GII.4 v0_2000, GII.4 v2_2004 and GII.3 VLPs. P-
646 pAb= rabbit policlonal anti-serum raised against GII.4 VA389_1996 P particles.
647

648 Table 4. 3C3G3 epitope sequence in different variants of the GII.4 norovirus.
649

Norovirus strain (variant)	Accession number	Year	Amino acid residues of norovirus VP1 (2006b Den Haag)											Antigenic site B
			245	247	389	390	397	435	443	444	445	446	448	393-395
3C3G3 epitope			P	E	I	Q	R	R	G	Y	P	N	D	
GII.4 MD134-7 (<1996)	AY030098	1987	-	-	-	-	Q	-	-	-	-	-	N	D - H
GII.4 Bristi (<1996)	X76716	1993	-	-	-	-	Q	-	-	-	-	-	N	D - H
GII.4 Kaiso (<1996)	AB294779	2003	-	-	-	-	Q	-	-	-	-	-	N	D - R
GII.4 VA387 (1996)	AY038600.3	1998	-	-	-	-	Q	-	-	-	-	-	N	N - N
GII.4 004 95M-14 (1996)	AF080551	1995	-	-	-	-	Q	-	-	-	-	-	N	N - N
GII.4 Narita 104 (1996)	AB078336	2002	-	-	-	-	Q	-	-	-	-	-	N	N - N
GII4 V0 (1999)		1999	-	-	-	-	Q	-	-	-	-	-	N	N - N
GII.4 Farmington Hills (2002)	AY502023	2002	-	-	V	-	Q	-	-	-	-	-	N	N G T
GII.4 Oxford B5S22 (2002)	AY581254	2003	-	-	V	-	Q	-	-	-	-	-	N	N G T
GII.4 Hunter 284E (2004)	DQ078794	2004	-	-	V	-	-	-	-	-	-	-	-	S T T
GII4 V2 (2004)		2004	-	-	T	-	-	-	-	-	-	-	-	S T A
GII.4 Kimitsu (2004)	AB294784	2005	-	-	V	-	Q	-	-	-	-	-	N	S T T
GII.4 Den Haag 54 (2004)	EF126962	2006	-	-	V	-	Q	-	-	-	-	-	N	S T T
GII.4 Isumi 060936 (2006a)	AB294790	2006	-	-	V	-	Q	-	-	-	-	-	N	S T T
GII.4 Yerseke 38 (2006a)	EF126963	2006	-	-	V	-	Q	-	-	-	-	-	N	S T T
GII.4 Sakai (2006b)	AB220922	2005	-	-	-	-	Q	-	-	-	-	-	N	S S A
GII.4 NSW696T (2006b)	EF684915	2006	-	-	T	-	-	-	-	-	-	-	-	S T T
GII.4 Den Haag (2006b)		2006	-	-	-	-	-	-	-	-	-	-	-	S T T
GII.4_Apeldoorn (2007)		2007	-	-	-	-	-	-	-	-	-	-	-	N T A
GII.4 New Orleans (2009)	KR904211	2009	-	-	-	-	-	-	-	-	-	-	-	G T T
GII.4 Sydney (2012)	AGV76572.1	2012	-	-	-	-	-	-	-	-	-	-	-	S T T

650

651 **Figure 1.** Alignment of the deduced amino acid residues from GII.4 VA387_1996,
652 M1 to M5 mutants and the Den Haag_2006b variant. The eleven residues forming the
653 predicted 3C3G3 epitope are boxed (R397 and D448 in red).

654

655 **Figure 2.** 12% SDS-PAGE gel stained with Coomassie blue showing the 10 different
656 P particles used in the present study. The molecular weights are indicated with bars on
657 the left of the image.

658

659 **Figure 3.** Chromatograms showing the size exclusion chromatography of GII.4
660 VA387_1996, M1 to M5 mutants and Den Haag_2006b P particles (panels A to G).
661 The arrows indicate the elution peak corresponding to P particles with an expected
662 molecular weight of 840 kDa. The asterisks show the elution peak of non-particulate
663 proteins. The elution times and calculated molecular weights of each P particle
664 preparation are indicated in panel H.

665

666 **Figure 4.** Binding properties of 4 different antibodies: anti-v0.8, anti-v2.5, 3C3G3
667 and HPA pAb to a panel of norovirus antigens (VLPs, P particles and P domain)
668 analysed by ELISA. For clarity, only the 1/1,000 dilutions are represented. The error
669 bars indicate the standard deviation of three replicates. The horizontal line indicates
670 the cut-off value of the ELISA.

671

672 **Figure 5.** Blockade of GII.4 Den Haag_2006b P particles binding to a secretor
673 positive saliva by the 3C3G3 mAb. The error bars indicate the standard deviation of

three replicates. The numbers in the X axe indicate the concentration of the 3C3G3 mAb.

Figure 6. Structural models shown in surface of the different mutants produced in the present study. The P1 subdomain is shown in gray and the P2 in blue. Blood group trisaccharide type A was located according to PDB id: 2OBS and can be found as a stick representation. Panel A shows the structure of VA387_1996 wild type with the residues forming the 3C3G3 epitope in red. Panels B, C and D show the single mutants M1, M2 and M3, respectively. Panel E shows the model of the double M4 mutant and panel F the model of the M5 multiple mutant. All mutations are shown in pink. Only mutant M5 has the D448 anionic carboxylate (RCOO−) and R397 cationic ammonium (RNH3+) in a close conformation that increases the possibility of a saline bridge formation that allows the 3C3G3 epitope stabilization.

Figure 7. Binding of different antibodies to wild-type and mutant P particles analysed by ELISA. Panel A shows the recognition by the P-pAb and 3C3G3 antibodies. Panel B shows the recognition by anti-v0.8 and anti-v2.5 mAbs. Only the 1/1,000 dilution is shown for clarity. The error bars indicate the standard deviation of three replicates. The horizontal line indicates the cut-off value of the ELISA.

Figure 8. Representation of the different affinity constants (KD) in molar (M) obtained by surface plasmon resonance experiments. The error bars indicate the standard deviation of three replicates. The arrow indicates the better interaction pair.

698 **Figure 9.** Percentages of binding of seven different P particles (VA387-1996, M1 to
699 M5 and Den Haag_2006b) to five different HBGAs (SiLe^x antigen, Le^x antigen, blood
700 group A, B and O (H) antigens) determined by ELISA. Each P particle binding was
701 normalized with the higher OD_{492} value, and percentages are shown. Error bars
702 indicate the standard deviations. Human serum albumin (HSA) was used as the
703 control.

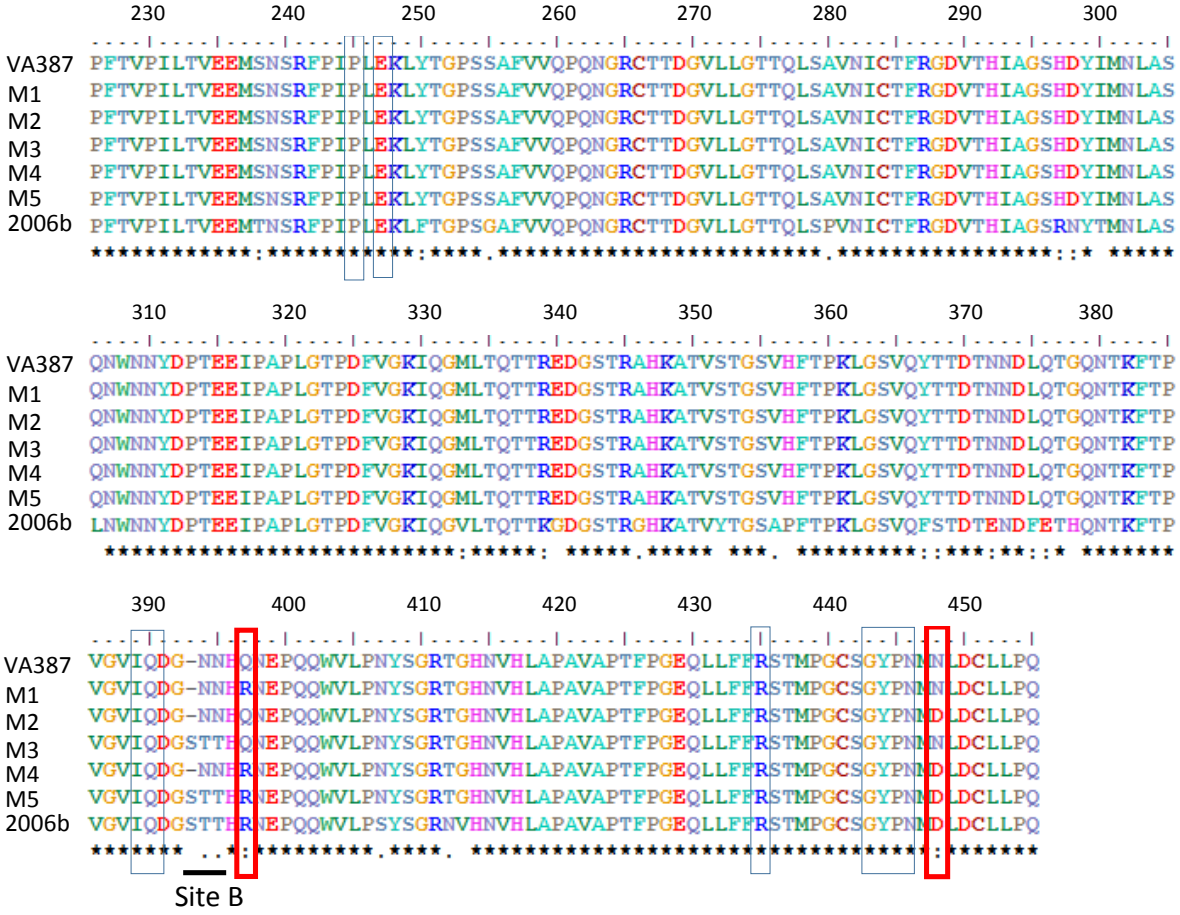

Figure 1

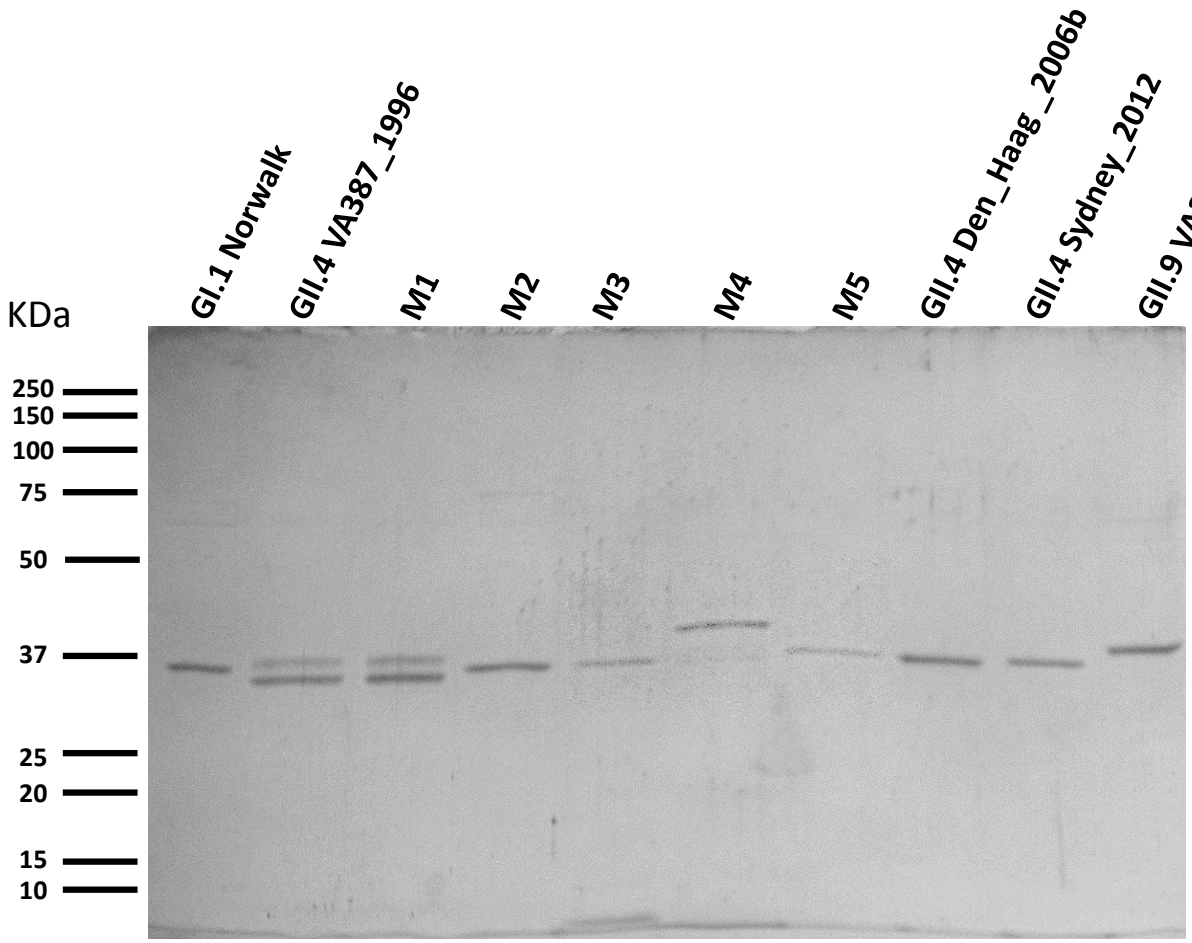

Figure 2

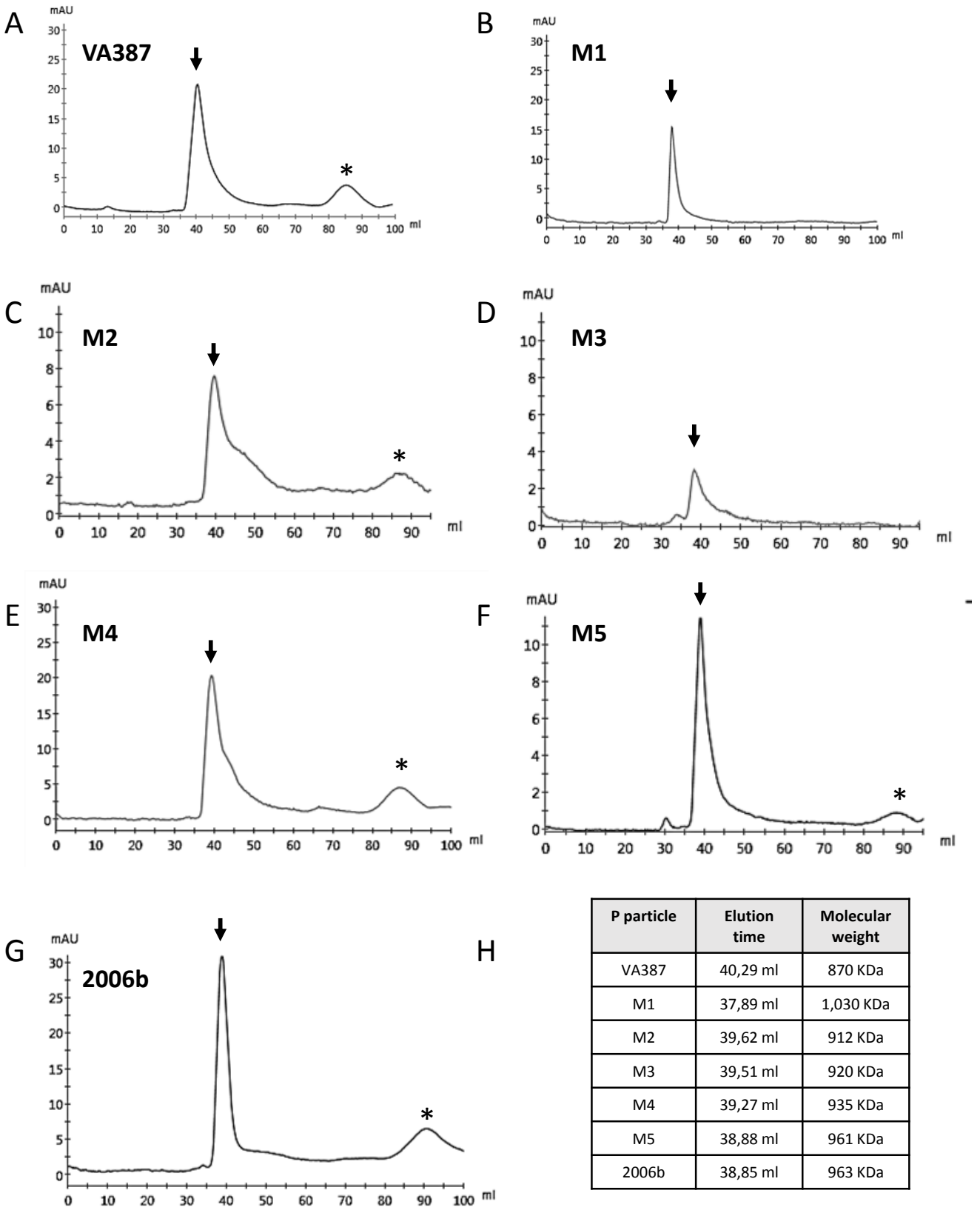

P particle	Elution time	Molecular weight
VA387	40,29 ml	870 KDa
M1	37,89 ml	1,030 KDa
M2	39,62 ml	912 KDa
M3	39,51 ml	920 KDa
M4	39,27 ml	935 KDa
M5	38,88 ml	961 KDa
2006b	38,85 ml	963 KDa

Figure 3

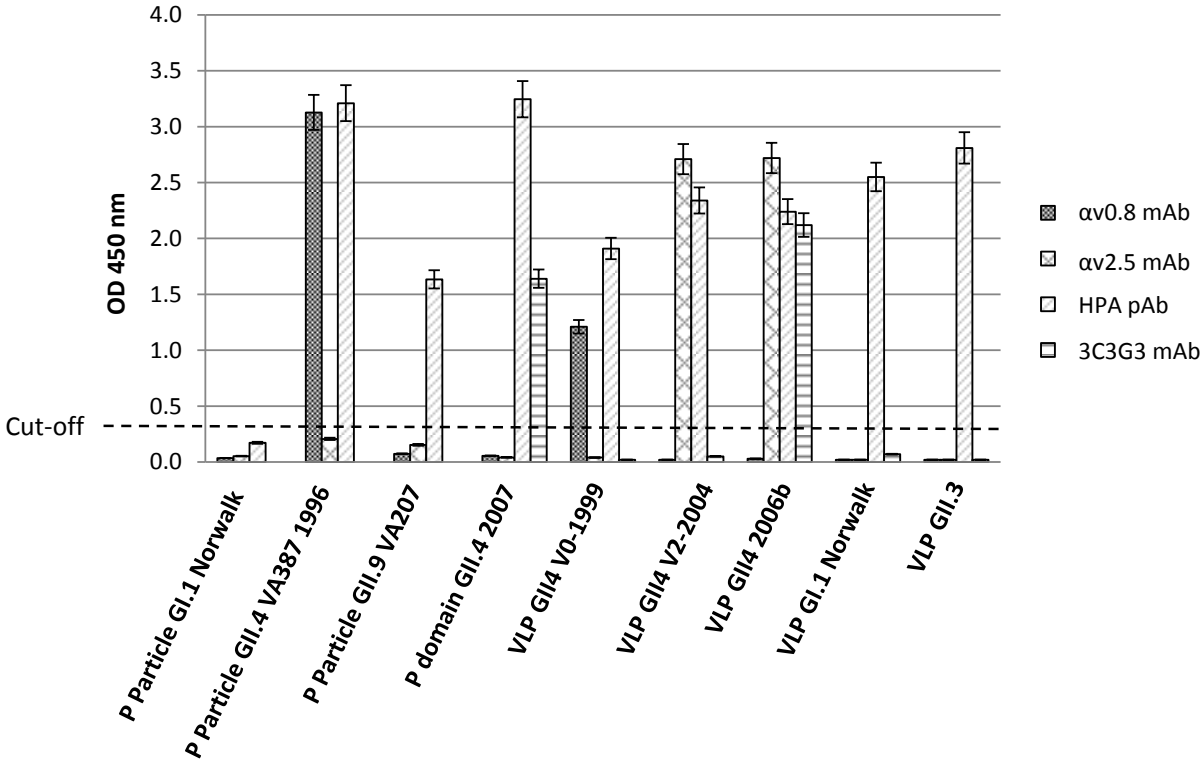

Figure 4

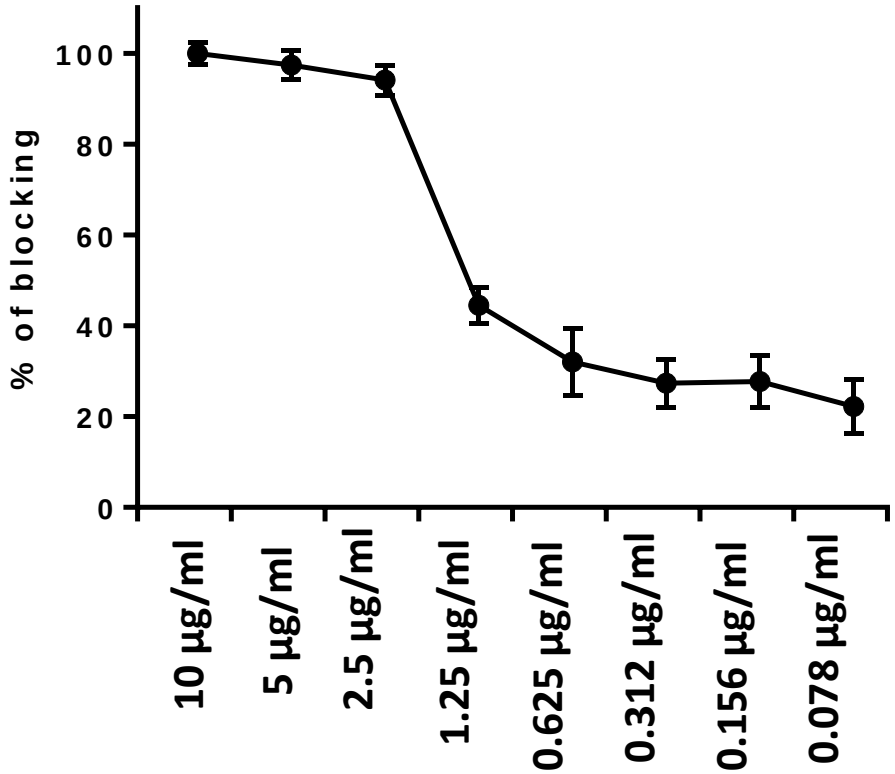

Figure 5

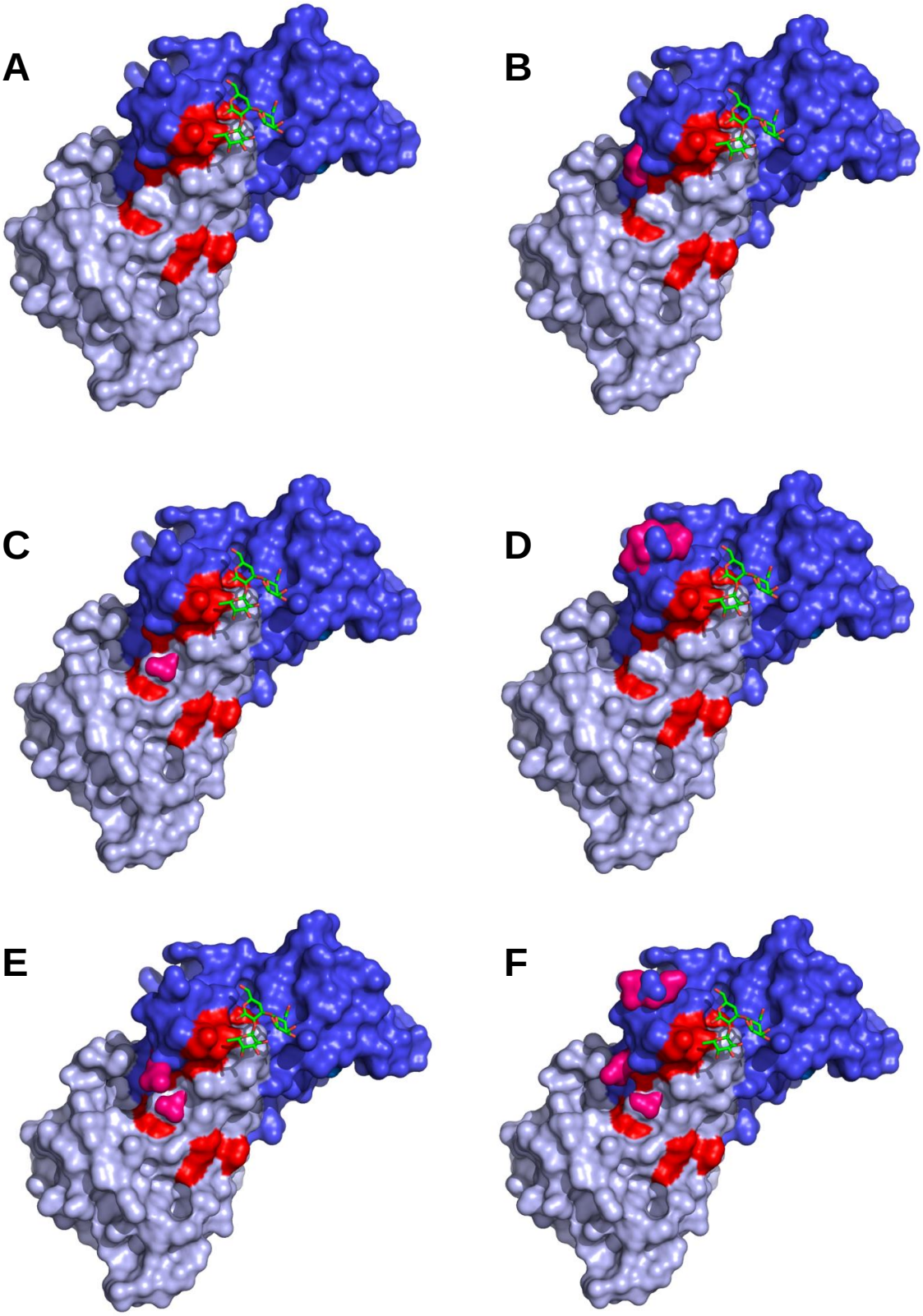

Figure 6

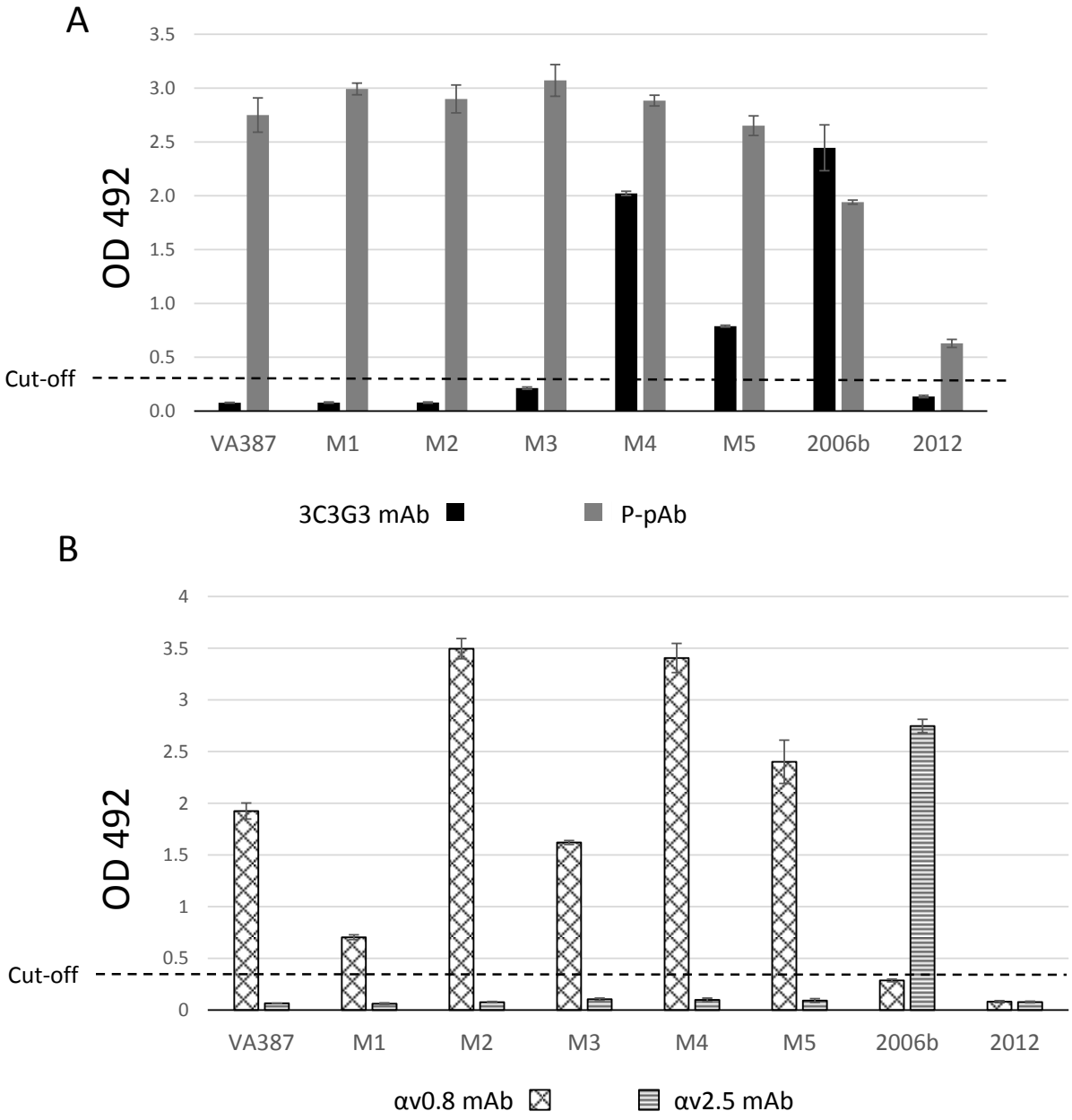

Figure 7

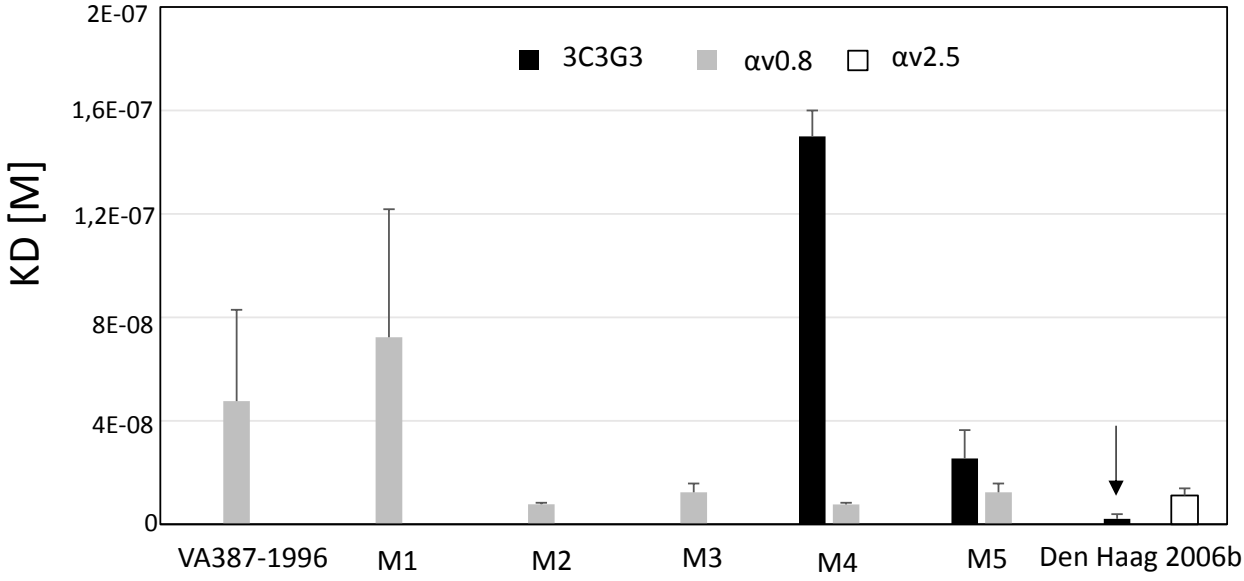

Figure 8

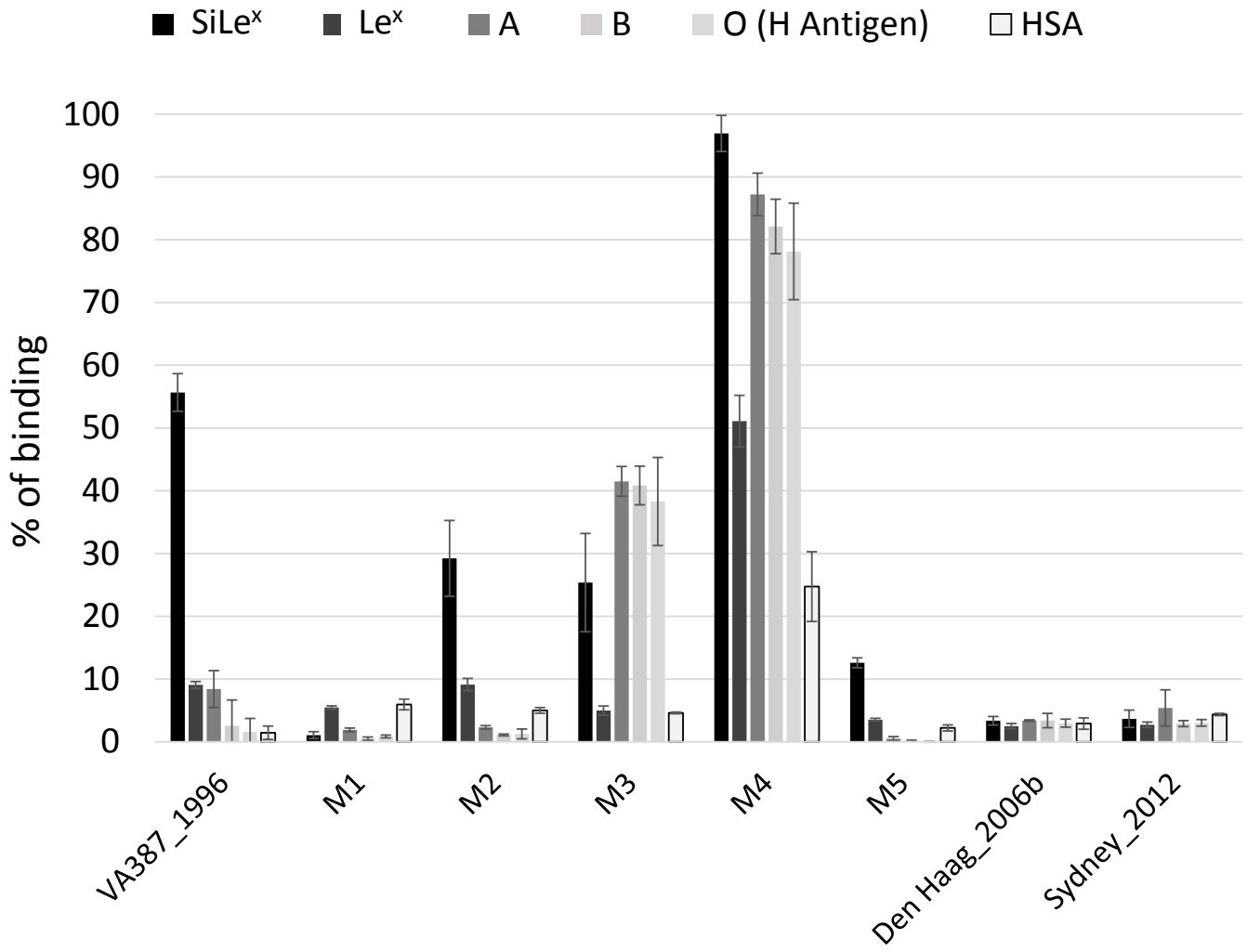

Figure 9